Pharmacology 2020 :Azadiradione ameliorates neurodegenerative diseases in mouse and fly models by potentiating DNA binding activity of heat shock factor 1 - Vinod Kumar Nelson- Jawaharlal Nehru Technological University

Dr Vinod Kumar Nelson
Raghavendra Institute of Pharmaceutical Education and Research, Anantapur, India

ABSTRACT
Toxicity associated with protein aggregation in the brain underlies various neurodegenerative diseases (NDs) such Parkinson's diseases, and polyglutamine based diseases such as Huntington's diseases, and spinocerebeller ataxias. It has been shown that heat shock response (HSR) that maintains cellular protein homeostasis in response to protein unfolding is defective in these diseased conditions. Consistently, upregulation of activity of heat shock factor (HSF1), the central regulator of HSR and expression of its target protein chaperone genes through small molecule or overexpression, respectively yielded promising results in both cell and animal disease models. However, all small molecule activators of HSF1 reported thus far functions indirectly. We have isolated azadiradione (AZD) by HSF1-sensitive cell based reporter screening of extracts of seeds of *Azadirachta indica,* a plant known for its many medicinal properties. We show that AZD, a triterpinoid ameliorates toxicity due to protein aggregation and associated disease pathologies and symptoms in cell, mouse and fly models with all these activities correlating with activation of HSF1 function and expression of its target protein chaperone genes. Notably, HSF1 activation by AZD we report here is independent of cellular HSP90 chaperone or proteasome function. Furthermore, we show that AZD directly interacts with purified HSF1 with high specificity facilitating its binding to its recognition sequence with higher affinity. These unique findings qualify AZD as an ideal lead molecule for consideration for drug development against NDs that affect millions worldwide.

Introduction:
Neurodegenerative diseases (NDs) like Parkinson's disease, and poly-glutamine (polyQ) based diseases affect millions of people worldwide 1, 2. There is no cure; current treatment options only offers disease specific management strategies such as neuroleptic and antipsychotic drugs for temporary relief of disease symptoms 3, 4. to remove the protein aggregates 13. Involvement of a ribonucleoprotein complex in the function of HSF1 including its trimerization has been demonstrated 14, 15. Chemical inhibition of HSP90 and proteasome also results in HSF1 activation 12, 16.
Reduction of protein aggregates and its associated toxicity and disease symptoms by forced upregulation of HSF1 activity has shown a promising therapeutic avenue to treat the diseases of protein conformation 17. Several small molecule HSF1 activators have been reported through screening small molecule libraries and/or natural products 3, 18. Given the severity of disease burden on the patient and the society, compounds with novel and unique functional mechanisms are desired to explore a better treatment option.
We report here AZD as an inducer of HSF1 through screening of methanolic extracts of Azadirachta indica seeds by cell based activity assay coupled purification approach. Azadirachta indica, locally known as neem has been in use in the traditional medicine for treatment of many diseases including anti-inflammatory, anti-anxiety, and enhancement of cognitive ability 19, 20. We show here that AZD ameliorates paraquat induced Parkinson's symptoms in mice and polyQ protein induced damage in the eyes of fruit flies. The effects on the model animals were correlated with AZD induced HSP expression in the relevant organ in the animals. Notably, we find that this compound enhances the HSF1 activity by facilitating formation of its DNA binding competent form and without involving the proteasome or HSP90 chaperone.

Materials and method
Paraquat dichloride (PQ; 1,1'-Dimethyl-4,4'-bipyridinium dichloride hydrate), Celasterol, Geldenamycin and Bortezomib were purchased from Sigma Aldrich, Inc. (St. Louis, MO); α- synuclein, tyrosine hydroxylase (TH), Raf1, Poly-ubiquitin antibodies were procured from Cell Signaling Technology, Inc. (Danvers, MA, USA); α-HSP70, α-β-actin antibodies were from AbCam. The secondary

antibodies goat α-rabbit IgG–HRP (horseradish peroxidase) and rabbit α- mouse IgG–HR were purchased from GeNei Pvt. Ltd. (Bangalore, India). Reagents and developer kit for immuno-histochemistry were procured from vector labs, USA. FITC- conjugated secondary mouse anti-goat antibody was purchased from Santa Cruz biotechnologies (DA, USA). Other chemicals of analytical grade were purchased from SRL, Mumbai (India).

Extraction procedure

Selected neem seeds were purchased from local market in Kolkata. In brief, powder air dried 1 kg neem seeds was extracted with methanol (1.5L) by maceration method for one week. The extract was collected by filtering through cheese cloth followed by filtering through paper filter. The residual material collected on cheese cloth and filter paper was re-extracted with another round with the same amount of methanol for another week in the same manner. The extracts collected were pooled together and concentrated and dried by using rotary vacuum evaporator. Near about 100 g of crude methanol extract was obtained from one kg of dry powder. The crude extract was stored in the refrigerator until further processing.

Fractionation

Fractionation was guided by enhancement of specific activity of a fraction. Silica gel column (mesh size 230-400, bed volume 160 ml, L=25 cm, D= 4 cm) was used majorly to purify the desired activity where the mobile phase was chosen by checking the profile i.e., movement of the compounds on the thin layer chromatography (TLC) profile. That is, the solvent ratios in this case n-hexane, ethyl acetate ratio- that gave the best resolution of spots in a test TLC plate of the extract taken as mobile phase. For silica gel column the following solvents were used sequentially as mobile phase. (For 50 g of crude extract, 400 ml each of the following was applied hexane: ethyl acetate (H:E) 1:0, 8:1, 4:1, 3:1, 2:1, 1:1, and 0:1. For each mobile phase entire flow through (400 ml) were separately collected and dried in vacuum evaporator and tested for the HSF1 activation activity in the HCT116 reporter cells containing (6XHSE GFP Rluc). Chromatographic fractions collected in H:E= 4:1 fraction carried the most activity. The TLC profile of H: E=4:1 fraction has shown three major spots (visualized by using UV lamp and 10% H2SO4 (in methanol) charring solution). For further purification the fraction of 20 g was applied to another silica column. Here compounds were eluted with ~400 ml each mobile phase composed of H:E with ratio 6:1, 5:1, 4:1, 3:1, 2:1, 1:1, and 0:1. All fractions were separately collected, dried and tested for the activity. Activity was only located in H:E::2:1 fraction (180 mg). The TLC of the fraction showed a single major spot. Further purification of the compound carried out by HPLC (SHIMADZU SPD-20A) with C18 column, (dimension 4.6 X 250 mm). An isocratic mode was used with acetonitrile:water (60:40) as the mobile phase with flow rate at 1 ml/min (sample injection volume of 20 µl).

Identification of the compound

Analysis of 1H, 13C, NMR and HRMS (ESI mass) data as well as searching perfect match of these spectra with those of Azadiradione helped to conclude on the identity of the compound.

Cell culture

The mammalian cell lines used in this study were HCT116 stably transfected with 6X HSEGFP- RLUC, HEK293 FT, MEFWT and MEFhsf1-/- , and Neuro2a. All cells were grown in complete DMEM supplemented with 10% FBS (invitrogen), 1% L-Glutamine, 0.1 mM nonessential amino acid, and 100U/ml penicillin/streptomycin. Cells were maintained at 37ºC and 5% CO2 environment.

DPPH radical scavenging activity

DPPH radical scavenger assay was done by adding different concentrations (1 µM to 10 µM) of compound or ascorbic acid as positive control mixed separately to an equal volume of ethanol to finally add 50 µl of DPPH solution (1 mM). After incubation for 5 min at room temperature absorbance was taken in UV spectrophotometer at 517 nm.

Measurement of Intracellular ROS

HCT116 cells grown in 12 well plates to ~75% Confluency were treated with 10 µM arsenic, various concentration of AZD and DMSO (vehicle control) for 12h. After treatment cells were washed with PBS and incubated with 20 µM DCF-DA (which was dissolved in serum free media) for 30 mins at 37°C in dark. Then cells were washed, collected and analyzed by flow cytometry for fluorescence measurement. By selecting the fluorescent population in the cells the fluorescence intensity was calculated using the FACSuite software. The fluorescence intensity indicates the generated ROS inside the cell.

Cell viability assay

Neuro2a cells were plated in 96 well plate, 24h before treatment. At about 70% Confluency cells, were treated with different concentration of AZD or Celasterol or DMSO for 16 h. After treatments the media discarded and 50 µl of MTT solution (5mg/ml in phenol red free media) was added to each well incubated for 3h in dark at 37ºC. After incubation, MTT solution was removed, 100µl DMSO added and absorbance was taken at 590nm.

Luciferase assay

Cells grown in 24 well plates overnight to ~70% confluence were treated with different dosages of Azadiradione (AZD) for

16 h along with DMSO (vehicle control). After treatment cells were harvested with the thermo dual luciferase lysis buffer. Equal amount of WCE measured by Bio- rad assay were loaded in white flat bottom plate. Luciferase activity was measured by thermo dual luciferase assay kit in a luminometer (Perkin elmer victa).

Reverse transcription-PCR

Cells/tissue (treated as per experimental needs) were harvested and total RNA was isolated by Trizol reagent (Invitrogen) according to the guidelines of manufacturer. Reverse transcription reaction were performed from 1 µg of total RNA using the I script Bio-Rad cDNA synthesis kit. Semi-quantitative PCR were performed using various gene specific primers

Western blot

Whole cell extracts (WCE) were prepared in RIPA lysis buffer (25 mM Tris-HCL pH 7.4, 150 mM NaCl, 1 mM EDTA, 1 mM EGTA, 1% NP-40, 1% sodium deoxycholate, 2.5 mM sodium pyrophoshphate 1 µg/ml leupeptin, 1 µg/ml aprotonin, 1 µg/ml pepstatin A). 20 µg of the WCE was loaded on 10% SDS-PAGE gels and transferred to PVDF membrane. The membrane was then blocked with 5% BSA for 30 mins and then probed with following primary antibodies.

Electrophoretic mobility shift assay (EMSA)

EMSA was done using 32P-γ-ATP labeled probe containing the proximal heat shock element (HSE) from the human hsp70A1A promoter. Binding reaction were performed with 20 µg of WCE purified from treated or mock treated (as per experimental needs) HEK293 cells stably expressing FLAG tagged HSF1 or with 0.5 µM of purified recombinant his6-tagged protein (prepared from over-expressing E. coli strain) in binding buffer (20 mM HEPES pH 7.4, 100 mM NaCl, 0.5 mM EDTA, 10% glycerol, 1 µg BSA, and 2.5 µg salmon sperm DNA) and 1 ng of the 32P-labelled HSE. Specificity of the binding was confirmed by competing the binding with 50X excess of specific (HSE) cold or nonspecific cold DNA oligonucleotides. Supershift reactions were performed by pre-addition of the antibody incubating the WCE with 1 µg of anti- FLAG antibody for 10 min on ice prior to the binding reaction.

Animal studies

Male Swiss albino mice ~25g were obtained from National institute of nutrition (NIN), Hyderabad and maintained in cages with bedding of wood flakes and straw in central animal research facility, Bose Institute under controlled environment [(23 ± 2°C), humidity (50 ± 5%) and 12 h of light and 12 h dark cycles. Mice were provided with flour and milk powder and filtered water ad libitum. All the animal experiments were conducted following "Principles of laboratory animal care" (NIH publication No. 85- 23, revised in 1985) as well as specific Indian laws on "Protection of Animals" under the provision of authorized investigators. The protocols were approved by the Institutional Animal Ethics Committee at the Bose Institute, Kolkata. (Ref no. IAEC/BI/2/2015).

PQ administration and Drug treatment

Male Swiss albino mice (n=25) were separately caged for the experimentation purpose. Among them 15 mice intraperitoneally (i.p) received injection of PQ at a sub-lethal dose of 10 mg/kg body weight twice a week for 4 weeks. Mice were then randomly divided into 4 groups of five in each comprising (A) saline treated for initial four weeks and continued for rest two weeks (n = 5)

(B) mice randomly chosen from above mentioned PQ-treated stock treated saline for next two weeks (C) mice randomly chosen from above mentioned PQ-treated stock and administered Azadiradione (AZD) for two weeks at 10 mg/kg body weight (D) like (A) but treated last weeks with AZD instead of vehicle for two weeks at 10 mg/kg body weight.

Immuno-histochemistry

Paraffin-embedded brain tissues were processed for microtome sectioning to obtain 10 µM thick sections. The sections obtained from various samples were then processed for immunohistochemistry using the reagents from vector laboratories. In a nut-shell, after de- paraffinization in xylene, antigen retrieval is performed for 45 min at 70ºC in a water-bath. The sections were then quenched, permeabilized, blocked and then incubated with the tyrosine hydroxylase antibody at a dilution of 1:500 for 16 h at 4°C in a humid chamber. Biotinylated secondary antibody (1: 500) was then applied. The signal was enhanced by the ABC kit and developed using ImmPACT Novored Peroxidase Substrate. Stained sections were imaged using bright-field microscopy on a Leica DM RXA2 microscope. All images were captured at 10 x and 100x magnifications.

Fruit Fly stocks

Oregon R+: Wild type strain of Drosophila melanogaster w1118; GMR-GAL4 (Freeman 1996): This is a homozygous viable transgenic line in which the yeast Gal4 gene is downstream of a multimerized copy of the binding site of the Drosophila Glass transcription factor. Glass multimer reporter (GMR) is expressed in all differentiating cells posterior to the morphogenetic furrow in the developing eye discs44 (Ellis et al 1993). The transgene insertion is present on chromosome 2. w1118; UAS-127Q (Kazemi-Esfarjani and Benzer 2000): This is a transgenic line in which a 127 CAG trinucleotide repeat unit, flanked by a HA tag, has been placed downstream of the UAS promoter. The transgene insertion is on chromosome 2 and is homozygous viable without any apparent phenotype. The stock was obtained from Dr. Parsa Kazemi-Esfarjani (University at Buffalo, New York). For examining the external morphology of adult eyes following feeding on AZD supplemented or

regular food, flies of the desired genotype were etherized and their eyes were photographed using a Sony Digital Camera (DSC-75) attached to a Zeiss Stemi SV6 stereobinocular microscope

Nail polish imprints

A transparent nail polish was used to create an exact replica of the external surface of the eye, which was subsequently examined by DIC microscopy (Arya and Lakhotia, 2006). The flies to be examined for eye morphology were anaesthetized, and decapitated with a sharp blade or needle. The decapitated head was briefly dipped in a drop of transparent nail polish. The head was then placed on a clean and dry area of the same slide and the nail polish layer was allowed to dry at RT for 5-10 min. The dried layer of nail polish was peeled off from the eye with the help of fine dissecting needles. The separated peel, being an exact replica of the eye surface, assumed a goblet shaped appearance. The peel was carefully placed on another clean glass slide with the imprint side facing up and carefully flattened by gently placing a cover slip over it and by applying a slight pressure, if required. The eye imprint was then examined under a microscope using 20X differential interference contrast (DIC) objective as described by Arya and Lakhotia (2006).

Phototaxis Assay

This assay was performed with a Y maze, a Y shaped glass tube of 12 mm diameter and 30 cm length of each arm. Two arms of the Y maze were covered with black paper to make dark and residual arms while one arm was left uncovered to serve as light chamber. The 1 day, 5 days and 10 days old flies of desired genotype were subjected to the phototaxis assay for 1 min and the total numbers of flies in each arm were counted (Dwivedi et al 2013). At least three trials were performed for each assay and the experiment was done in several replicates of 10 flies each indicated in results section.

Microscopy and image analysis

For recoding the external morphology of adult eyes, flies of the desired genotype were etherized and their eyes photographed using a Sony Digital Camera (DSC-75) attached to a Zeiss Stemi SV6 stereobinocular microscope for examining the external morphology of adult eyes.

For light microscopy, a Nikon E800 microscope was used with appropriate filter combinations. The images obtained were recorded with a Nikon DXM 1200 digital camera. The different objectives used were 10X (0.3NA, Plan Fluor), 20X (0.5NA, Plan, Fluor) or 60X oil (1.4NA, Plan, Apo).

Expression and purification of human HSF1protein

An expression construct pET15 carrying a codon optimized HSF1 cDNA tagged with DNA encoding a hexa-histidine peptide was used to produce the protein in E. coli BL21 (λDE3) cells with standard IPTG induction protocol. The induction was carried out (with 1 mM IPTG) at 15˚C for 16 h). Cell pellet was lysed in ice cold lysis buffer (50mM HEPES, pH 7.5), 300 mM sodium chloride, and supplemented with 20 mM imidazole, 0.5 mM PMSF by sonication. The his6- tagged HSF1 was bound on the NTA beads by incubating cleared cell lysate in a batch method. Beads were washed several times with wash buffer lysis (buffer with 40 mM imidazole). Finally bound protein was eluted in elution buffer (lysis buffer supplemented with 250 mM imidazole). The eluates pooled together were dialyzed against the lysis buffer without imidazole, flashed freezed in aliquotes and stored in -80°C for future use.

Spectral Measurements

Absorbance measurements were performed in a JASCO (Tokyo, Japan) V-530 UV-visible spectrophotometer equipped with a Peltier temperature control system, using a cuvette of 1cm path length. All fluorescence measurements were performed using a fluorescence spectrophotometer (Photo Technology Inc. USA, Model QM-4CW) equipped with a Peltier temperature control system. Fluorescence data was corrected for the inner filter effect F=Fobs X antilog [(Aex +Aem) /2] where Aex is the absorbance at the excitation wavelength and Aem is the absorbance at the emission wavelength

Florescence study

Azadiradione and HSF1 interaction

The binding of the ligand to the protein was monitored by enhancement of protein fluorescence in the presence of ligand. Ligand (0-10 µM) was titrated with fixed concentration of HSF1 (2 µM) at room temperature. The excitation wavelength was 280nm and emission wavelength range was set to 310 nm to 400 nm. The dissociation constant Kd could be calculated from the Scatchard plot according tor / Lfree = (r /Kd)–(n/Kd) Where, r is the ratio of the concentration of bound ligand to the total protein concentration and n: represents the maximum number of binding sites. The binding of the ligand to the protein was also studied under different condition. We first pre- incubated HSF1 (2 µM) at 42ºC for minute to allow trimerization and then measure the fluorescence of that trimerize HSF1 by titrated with ligand (0-10 µM) at room temperature. In another condition we pretreated HSF1 (2 µM) with 1mM DTT at room temperature and then measure the fluorescence of protein by titrated with ligand (0-10 µM) at room temperature.

We also determine the binding of the ligand to the HSF1 was specific or not. For this ligand (0- 10 µM) was titrated with fixed concentration of lysozyme or Hsp90 (2 µM) at room temperature. For check the validity of our study we titrated known Hsp90 inhibitor compound with fixed concentration of Hsp90 at room temperature.

Molecular Modeling and Docking

The DNA binding domain of HSF-1 is docked with another two similar domains to form protein-protein docked trimeric structures. The trimeric HSF-1 form was then docked with the double helical DNA with nucleotide sequence 5'-GGCGAAACCCCTGGAATATTCCCGACCTGGCAGC using Z-Dock server. DNA protein complex then was docked with Azadiradione in Glide module using standard precision (SP) mode (Glide, version 5.5, Schrodinger, Inc., New York, NY, 2009). The grid was prepared covering the entire structure of DNA with dimensions of 80×80×80 Å.

Adaptive Poisson-Boltzmann Solver (APBS) calculations

The electrostatic charge distributions of the protein were calculated using Electrostatic potential surface tools in Schrodinger. Atomic charge distribution, dielectric properties and electrostatic properties of protein can be well correlated using this model. The solute and solvent dielectric constant used for Poisson-Boltzmann settings were 1 and 80 respectively. The calculation for coulombic surface area is carried out at 298K

Results

Identification in and purification of Azadiradione from neem seeds as an activator of HSF1 by cell based reporter assays

Screening for activator of HSF1 was carried out by using cell based reporter system harboring both renilla luciferase (Rluc) and GFP independently under the control of six tandem copies of HSF1 recognition sequence called heat shock elements (HSE) (6XHSE) 21, 22. Incubation of the reporter cell with the methanolic extract of neem seeds resulted in the activation of both GFP and Rluc in a dose dependent manner (Fig. 1A). To understand the nature of the compound the activity was purified by resolving the sample through several rounds of silica gel columns using solvents of various polarities. The purification was verified by increase in the specific activity by Rluc assay down the purification steps (Fig. 1A). Finally, active molecule was purified; the compound obtained was found to be more than 95% pure judged by thin layer chromatography (TLC) and high performance liquid chromatography (HPLC) analyses. Electrospray ionization (ESI) mass spectrometer indicated the mass of the compound to be 450.7953 Dalton (Fig. S1A- C). The molecular structure of the compound as azadiradione (AZD) was confirmed by analyzing the data obtained by ESI mass- and 1H and 13C NMR spectroscopy as well as analytical HPLC analysis (Fig. 1B, S1A-C)

Azadiradione induces HSF1 activity in the cells

Hyperphosphorylation-, ability to bind the HSE, and activate transcription of chaperone genes are signatures of HSF1 activation process 23. To test on the activity of HSF1, whole cell extract (WCE) of HEK293 cells pre-treated with AZD or DMSO or heat shock (HS) as positive control were prepared. The HEK293 cells carried a stably expressed FLAG-tagged HSF1. As revealed by electrophoretic mobility shift assay (EMSA), WCE treated by AZD or HS induces HSE binding to a comparable level relative to DMSO treated samples (Fig. 1C, compare lanes 1-3 &7). Formation of a supershifted complex by addition of anti-FLAG antibody indicated the presence of FLAG-HSF1 in the shifted complex (Fig. 1C, compare lanes 3&5, and 7&9).

Immunoblot experiment find that HSF1 was also hyperphosphorylated in the AZD treated WCE as revealed by a relative slower mobility of HSF1 in the SDS-PAGE compared to DMSO treated counterpart that collapsed to a single relatively faster moving species alike DMSO treated samples by phosphatase (CIP) treatment (Fig. 1D). Transcriptional activation of HSF1 by AZD treatment was confirmed by determining the increased expression of the inducible hsp70A1A (noted as HSP70 in all subsequent experiments with HSP70A1A) and HSP27 in dose dependent manner. AZD responsiveness in a cell is sensitive to its shRNA-mediated HSF1 knock down (Figs. 1E-F). Failure of induction of HSP70 in mouse embryonic fibroblast (MEF) cells with HSF1 gene knocked out

(MEFhsf1-/-) but wild type MEF (MEFwt) cells confirmed that AZD acts through HSF1 (fig. S2A). Alike heat shock, AZD in a dose dependent manner provided cytoprotection against lethal heat shock stress (45ºC/1h (Fig. S2B)18, 24-26.

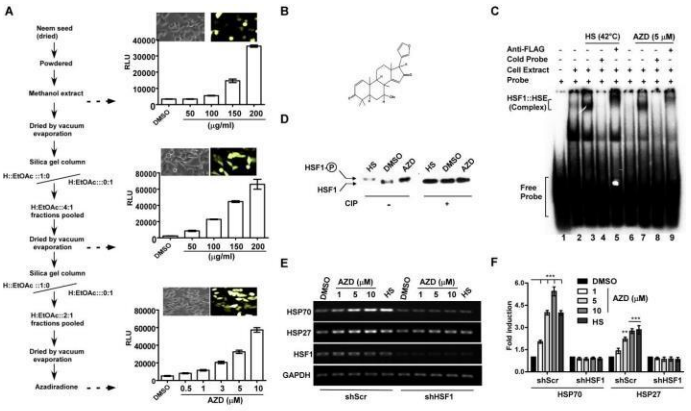

Figure 1: Azadiradione (AZD) activates HSF1 and its target heat shock chaperone genes. A) Flowchart of stepwise purification of AZD accompanied by increase in specific activity measured by GFP (next to phase contrast images of cells) and luciferase assays as indicated. H, n-hexane. B) Chemical structure of AZD. C) AZD induces

DNA-binding ability of HSF1 in cells determined by EMSA using radiolabeled HSE as described in the materials and methods. Whole cell extract (WCE) (50 µg) prepared from HEK293 cells stably expressing FLAG-HSF1 pre- treated with AZD at

indicated doses or DMSO or HS (at 42°C/1h) were used for binding to 32p-γ-ATP-labeled HSE DNA-oligo as probe (~ 1 ng/tube) in a volume of 25 µl on ice for 30 min. The reactions were resolved in a 4% acrylamide and bis-acryamide (29:1) gel, and autoradiographed. D) AZD treatment induces HSF1 hyperphosphorylation like HS in WCE used in (C) which was erased upon phosphatase treatment determined by immunoblot with α-FLAG antibody. E) AZD treatment induces HSP70 and HSP27 transcription like HS in HEK293 cells that is sensitive to shRNA-mediated HSF1 downregulation (shHSF1) compared to scramble (shScr) determined by RT-PCR assay. A representative agarose gel of PCR products obtained using equivalent amounts of cDNAs from cells treated as indicated stained with ethidium bromide. F) Densitometric quantitation of HSP70 and HSP27 bands in agarose gels as shown in panel E from three independent experiments.

Azadiradione reduces protein aggregate formation in cellular polyQ disease model.

Classical heat shock response (HSR) involves elevated expression of HSPs that is capable of refolding of unfolded/misfolded client proteins to prevent their aggregation in the cell 27. HSR can also activates proteasome that help clear cellular protein aggregates through ubiquitin dependent pathway 5, 16.

AZD was tested to reduce in concentration dependent manner the aggregation of an aggregation prone ataxin130Q protein expressed in mouse neuroblastoma (Neuro-2a) cells compared to vehicle treated samples. The activity was correlated with the induction of HSP70 expression level in Neuro-2a cells (Fig. 2A-C) 28. Results show the better effect of AZD in the applied concentration range than that of celastrol, whih inhibits bothe HSP90 as well as proteasome in resolving ataxin130Q protein aggregation as well as HSP70 expression 24, 29. Moreover, AZD was found to be relatively less toxic than celastrol based on MTT assay (Fig. 2D).

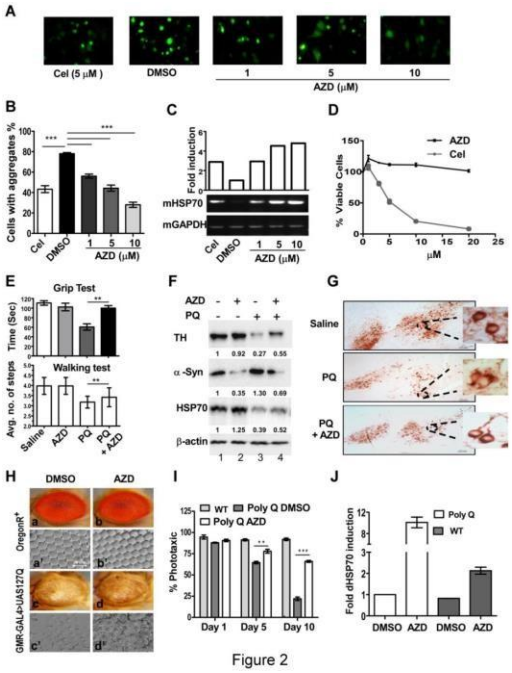

Figure 2: AZD reduces protein aggregation and associated toxicity in the cell, mouse and fly models. A) Effect on ataxin130Q-aggregation by AZD, or celastrol, or DMSO as indicated in Neuro-2a cells counted and plotted after 48 h treatment (B). C) Ethidium bromide stained agarose gel showing relative levels of HSP70 (mHSP70) transcripts (in cells represented in panel A) determined by semiquatitative RT-PCR assay. D) Sensitivity of Neuro- 2a cells to AZD was compared with celastrol in 24 h treatment by MTT assay. E) Reduction of Parkinson's symptoms in swiss albino mice (n=5) by AZD treatment for 2 weeks daily after PQ treatment given twice a week for 4 weeks (both used at 10 mg/kg body weight), F) Levels of tyrosine hydroxylase (TH), α-synuclein (α-syn), HSP70, and ß-actin in the WCE of substantia nigra (SN) isolated from the treated mice estimated by immunoblot. G) Levels of TH in the SN of mice determined by immunohistochemical staining. H) Dietary supplementation of AZD improved eye morphology (ac vs bd) and ommatidial arrays (a'c' vs b'd') damaged by 127Q expression in the eye of the fruit flies. I) 127Q induced damage in vision is reduced with AZD treatment assayed by phototaxis assay. J) HSP70 transcript levels estimated in the indicated samples by q-PCR.

Azadiradione restores the loss of dopermeniergic neuron induced by paraquat treatment in a mouse Parkinson's model

Aggregation of α-synuclein in the substantia nigra pars campacta (SN) and loss of dopaminergic neurons are common pathological markers in Parkinson's disease (PD). Loss of chaperone function and upregulation of chaperone activity were correlated with loss and restoration of dopaminergic neurons in the Parkinson's disease model, respectively 30, 31.

Because AZD activates cellular HSF1 and its target genes the effect of AZD treatment on PD symptoms was tested in mice model developed by treatment of the animals with paraquat (N,N'-dimethyl-4,4'- bipyridinium dichloride, PQ) 32. The development of PD and the efficacy of AZD on the reversal of PD symptoms was assessed by classical behavioral tests such as foot print- and grip tests along with assaying the levels of HSP70, α-synuclein and tyrosine hydroxylase (TH) in SN tissues in the treated vs untreated animals determined by immunoblot experiments. As shown treatment with AZD for two weeks after PQ administration for four weeks significantly reduced the PD symptoms estimated by these tests (Figs. 2E-G). AZD was also able to reverse the trend of body weight loss caused by PQ administration (Fig. S3A). Biochemical markers such as tyrosine hydroxylase (TH) for dopaminergic neurons, and α-synuclein levels were then estimated in the WCE isolated from the SN of the treated animals by immunoblot experiments. As shown loss of TH in PQ treated tissue is restored to a great extent by subsequent administration of AZD (Fig. 2F, lanes 3-4). AZD did not change the TH level in the SN relative to saline treated sample (Fig. 2F, lanes 1-2) but reduced the levels PQ-induced α-synuclein level (Fig. 2F, lanes 1-2 vs 3- 4). AZD treatment alone also caused net reduction in α-synuclein level (Fig. 2F, lanes 1-2). Immuno histochemical staining with TH antibody on the tissue sections prepared from brain showed restoration of lost dopaminergic neurons by more than 50% in agreement with biochemical data (Fig. 2G). Correlation of these results with elevated HSP70 levels (Fig. 2F, lanes 1-4) supported the notion that AZD treatment ameliorated the PD symptoms by induction of HSF1 and its target protein chaperone genes.

Effect of azadiradione on fruit fly model of poly-Q disease

Here protein carrying expanded poly-glutamine repeats (127Q residues) was overexpressed through eye specific driver construct GMR-GAL4-UAS-127Q in the larval eye imaginal discs of fruit flies. An overexpression of the protein resulted in the retinal degeneration and defective eye development in the adult fly (Fig. 2H-J). To test if AZD has any effect, fly larvae including oregonR+ types were grown on food supplemented with AZD or vehicle (DMSO) control from 1st instar larval stage to adult stage to test its effect on their retinal development. An effect of the treatments was analyzed by testing eye morphology, as well as architecture of ommatidial array in the eye captured as the nail polish imprints. While polyQ overexpression resulted in severe degeneration of retina including malformation of ommatidial units in the eye, AZD supplementation could rescue the damage to these structures to great extent (Fig. 2H: cd to c'd'). The fly larvae fed on either AZD or DMSO alone to grow to the adult stage developed normal eye morphology as well as normal ommatidial array architructure indicating AZD is not toxic to the flies (Fig. 2H, a vs b, and a' vs b'). To test if the partial recovery of the retinal damage through AZD treatment is due to induction of HSF1 activity, qPCR was carried out using the cDNA prepared from the total RNA isolated from 3rd instar larvae samples. Expression of HSP70 was significantly elevated in AZD treated samples suggesting that AZD reduced polyQ toxicity through induction of chaperones (Fig. 2J). Effect of polyQ induced toxicity in the retinal development was next examined by testing their vision by measuring the phototaxis ability of the flies to move towards light chamber from the dark chamber. Flies overexpressing polyQ fed on AZD or DMSO supplemented food from the 1st instar larval stage were subjected to phototaxis measurement at the age of day 1, day 5 and day 10 of adult fly. Comparison of phototaxis with their age matched counterparts showed that polyQ overexpressing flies progressively fall behind as they age in phototaxis compared to their normal counterparts but the polyQ overexpressing flies fed on AZD supplemented food acquired relatively improved phototaxis and vision 13 (Fig. 2I). At day 10, about 25% of flies overexpressing polyQ showed phototaxis which improved to 75% phototaxis through AZD treatment (Fig. 2I). Analysis of corresponding eye samples yielded elevation of HSP70 transcript with AZD treatment in normal as well as in polyQ expressing population (fig. 2J). AZD also induced HSP70 protein levels in different organs of the fly (Fig. S3B). Thus, AZD treatment restored polyQ induced damage in fly eye structure and function which are consistent with elevated expression of HSP70.

Azadiradione does not interfere with proteasome or HSP90 activity

Block of ubiquitin-proteasome and HSP90 activity results in HSF1 activation 13. These two apparatus perform essential cellular functions such as degradation of unfolded proteins to maintain cellular amino acid pool and chaperoning many essential cellular proteins including various signaling components such as Akt and Raf1, respectively 16. The majority of small molecule activators of HSF1 identified thus far induces HSF1 either by inhibition of proteasome or HSP90 or both 3.

To test the effect on proteasome function, HEK293 cells were treated with three doses of AZD, or DMSO or a known proteasome inhibitor bortazomib (as a positive control) for 16 h and estimated the extent of poly-ubiquitinated proteins (P-Ub) accumulated by immunoblot experiments. Relative inductions of HSP70 protein levels were also measured in those samples to correlate proteasome inhibition with the HSF1 activation (Fig. 3A). Comparison of relative proteasome inhibition versus HSP70 expression with bortazomib showed that proteasome activity in AZD treated samples is close to

DMSO treated samples whereas HSP70 protein level was induced in those treatments in dose dependent manner (Figs. 3A-B). Therefore, activation of HSP70 by AZD is not mediated through inhibition of the proteasome.

The sensitivity of HSP90 activity was carried out by treating HEK293 cells with different concentrations of AZD or DMSO, or geldanamycin, a known HSP90 inhibitor as the positive control for relative comparison of their activities (Fig. 3C). The sensitivity of HSP90 activity to AZD was determined in those treatments by estimating the relative stability of its client proteins such as Akt and Raf1 along with the HSP70 protein levels through immunoblot experiments. While levels of both the client proteins dropped significantly in geldanamycin treated WCEs, the WCE isolated from cells treated with increasing concentrations of AZD showed little change on the levels of those two HSP90 clients. Relative to geldanamycin treated sample the level of HSP70 protein was shown to be induced in the AZD-treated samples in dose dependent manner (Fig. 3C-D). Comparison of the levels of Raf1 and Akt with that of HSP70 protein (relative to DMSO) shows the extent of inhibition of HSP90 activity to activate the chaperone protein (Fig. 3C, compare lanes 1 and 2, and respective bar graphs in panel D). Therefore, elevation of HSP70 protein level in cell by AZD treatment is not mediated through the inhibition HSP90 activities.

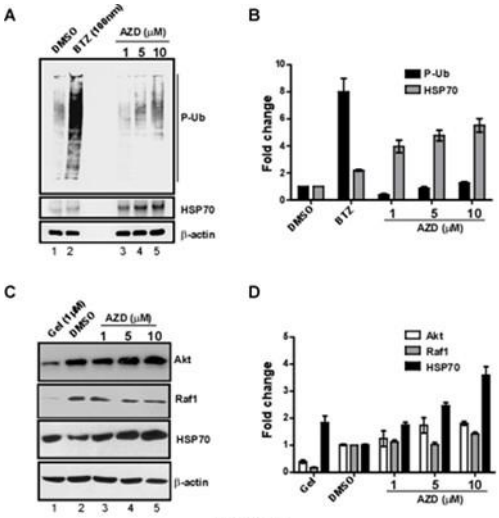

Figure 3

Figure 3: AZD induces HSP70 protein expression without interfering with the functions of HSP90 or proteasome. WCE (20 µg) of HEK293 cells pretreated for 16 h with bortazomib (BTZ) or geldanamycin (Gel) or various concentrations of AZD, or DMSO were subjected to immunoblot using the antibodies against (A) anti-polyubiquitin (P-Ub). The levels of HSP70 protein in the same samples were also determined as indicated using anti-HSP70 antibody. (B) The bands in the blot were estimated and plotted as bar graph considering ß-actin levels as an internal loading control. (C) Immunoblot with antibodies against two HSP90 client proteins Akt or Raf1, and HSP70 to compare their relative expression levels in those samples. (D) Band intensities in the blot were estimated by densitometric scanning and plotted to compare their expression levels. The band intensities in the blot were estimated and plotted as bar graph considering ß-actin levels as an internal loading control.

Azadiradione directly interacts and facilitates DNA binding ability of HSF1 protein Conversion of monomeric HSF1 present in the cytoplasm into a DNA-binding competent homotrimeric state is believed to an important step in its activation pathway 23. Purified HSF1 in vitro has also been shown to intrinsically form homotrimer competent of binding to its recognition sequence in response to heat shock or other stressful consitions 33-35. Important role of two cysteine residues in the DNA binding domain of HSF1 was demonstrated, because mutation in any of these residues impairs heat shock induced trimer formation by the protein 34. Based on our experimental results that AZD did not interfere with function of proteasome or HSP90 in the cell, it was a reasonable to check if it influence DNA binding efficacy of HSF1 (fig 3.)

To this end purified HSF1 was incubated with radio-labeled HSE (ds DNA oligonucleotide) either with DMSO alone or increasing concentrations of AZD to find that AZD increased the DNA binding of purified HSF1 in a concentration dependent manner by a gel mobility shift EMSA) experiment (Fig. 4A, lanes 1-3 and 6). The binding affinity was increased by more than 2 fold by the presence of AZD in the reaction. The specificity of the interaction was confirmed by elimination of the binding by addition of an unlabeled double stranded HSE in excess (lanes 3-4, and 6-7) but not by an unrelated dsDNA oligo of similar molecular weight (Fig. 4A lanes 3- 5 and 6-8). These results strongly suggest that AZD directly and with specificity facilitates DNA binding of purified HSF1 protein in vitro.

An effect of AZD addition on the binding of purified HSF1 to HSE was then re-evaluated by measuring the alteration of HSF1 (tryptophan) fluorescence in the presence of increasing concentration of HSE. There was little change of HSF1 fluorescence when a nonspecific oligo was present in the reaction (HSF1+Ns oligo) instead of HSE. The presence of AZD on the other hand enhanced quenching of HSF1 fluorescence by HSE in a concentration dependent manner (fig. 4B). Analysis of the data yielded dissociation constant (kd) of 0.8 µM of HSE-HSF1 complex versus 0.35 µM when AZD was present in the reaction (HSF1AZD-HSE) (figs. 4B-C, S4). Alteration of HSF1 fluorescence in the presence of AZD without HSE was measured to test if AZD can bind HSF1 alone. Surprisingly, an addition of AZD to a fixed concentration of HSF1 enhanced its fluorescence intensity in concentration dependent manner. An

induction of a blue shift in the emission maxima with increasing AZD concentration suggested a conformational change in the HSF1 protein with AZD binding (Fig. 4D, S5A). The change is HSF1 specific because AZD at the same concentration range did not alter fluorescence of HSP90 unlike geldanamycin did (Figs. 4E-F). AZD also did not alter fluorescence intensity of another unrelated protein lysozyme in the same concentration range (Fig. S6). The stoichiometry and the dissociation constant (kd) of HSF1-AZD interaction was estimated by analyzing these data in a Scatchard plot as 1.35 µM with a stoichiometry of one AZD per molecule of HSF1 protein r (Fig. 4D, inset).

Structural change in HSF1 protein with addition of the compound was also tested by recording the far-UV CD spectra; plot of negative elipticity versus wave length showed a net decrease in α- helical content in the structure by more than 6 % compared to 4% by heat shock. Random coil content in the protein was found to be increased by more than 5% by AZD treatment compared to 2% by heat shock (Fig. S5B and table S1). Heat shock was shown to induce oligomerization of HSF1 as an intermediate in its activation pathway 34. We find that AZD in a dose dependent manner induced oligomerization of HSF1 like heat shock as determined by measuring light scattering intensity at 350 nm (Fig. 4G). Interestingly, the oligomerization of HSF1 induced by AZD and heat shock was abolished in the presence of DTT in the reaction (Fig. S8A-C). Dynamic light scattering (DLS) analysis induced by AZD also indicated oligomerization of HSF1 protein (Fig. S7).

Figure 4: AZD directly interacts with the purified HSF1 protein tested by EMSA and fluorometric assay (A) Concentration-dependent enhancement of HSE binding of HSF1 (2 µM) by AZD that is competed out by excess unlabeled HSE (SpCold) but not by an unrelated double stranded (ds) DNA oligonucleotide (NSpCold) determined by EMSA as described in the method. B-C) Effect of AZD on binding of HSE by HSF1 measured by fluorometric assay. B) Effect of AZD (6 µM) on HSF1 (2 µM) by increasing concentrations of HSE indicated (NsOligo, non specific oligo=NSpCold). (C) Bar diagram representing the kd values of HSF1 binding to DNA without or with AZD. D) Concentration dependent effect of AZD as indicated on HSF1 (2 µM) (inset: Scatchard plot of AZD binding to HSF1) but (E) did not affect fluorescence of HSP90 (2 µM) protein while (F) Effect of geldanamycin in the indicated concentration on HSP90 fluorescence. (G) Concentration dependent effect of AZD (as indicated) and heat shock (HS) on HSF1 (2 µM) multi-merization in cell-free system determined by monitoring the kinetics of polymerization by using light scattering at 350 nm. The presence of DTT in the reaction abolished the polymerization induced by AZD or HS. H) Cartoon proposing AZD targeting free pool of monomeric HSF1, an intermediate between repressive and active HSF1 in the cell due to low level basal activity of HSF1 in a healthy cell to convert into active trimer state.

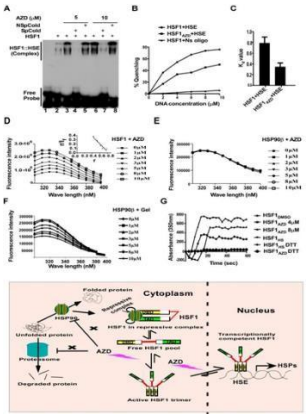

Discussion

Medicinal plants have been used to treat various diseases in traditional branch of medicine with largely unknown principle of action. Here we discussed our isolation of AZD from Azadirachta indica (neem) as an activator of cellular HSR as measured by upregulation of HSF1 activity. Treatment with AZD reduces protein aggregation and disease symptoms in cell, mouse and fly models. Neem has been in use in traditional medicine for more than 2000 years for its diverse medicinal properties including its role on neuroprotection and amelioration of Alzheimer's disease 20, 36. AZD activity reported here validated in principle its neuroprotective activity.

Evidence presented here support that AZD activates DNA-binding competence through stabilizing homomultimerization of HSF1 protein. This interaction of AZD, a triterpenoid with HSF1 is specific because AZD in the same concentration range and identical conditions did not interact with HSP90ß, or lysozyme (Figs. 4A-F, S7). No triterpenoids that were shown to activate HSP70 transcription such as celastrol or gedunin were shown to directly interact with HSF137. Moreover, AZD did not inhibit the cellular activities of proteasome or HSP90 to induce HSF1 activity under study. Our results also show that AZD induces ordered structural changes upon interaction with HSF1 as revealed by generating blue shift in the fluorescence emission spectra (Fig. S5A). CD analysis also revealed ordered structural changes in the HSF1 protein induced by AZD that is comparable to that caused by HS treatment (Fig S5B, table S1). These results therefore are consistent with the idea that interaction of HSF1 with AZD is highly specific.

Results are consistent with the idea that one molecule of AZD binds per molecule of purified HSF1 however the interaction mode apparently changes when the HSE is present in the

environment (Figs. 4D). One molecule of AZD binds per three molecules of DNA-binding domain of HSF1 (HSF1DBD homotrimer complex) as reveled by analysis of data by Scatchard plot (Fig. S9A). This also indicates that the C-terminal domain is not crucial for interaction with the compound. Molecular modeling also shows stabilization of trimer of HSF1DBD as a winged helix protein on the HSE through interaction with its asparagines and phosphate backbones of DNA (Fig. S9C). Docking of AZD altered salvation energy as well as eletrostatic charge distribution in the complex (Table S2) 38. A major hallmark of PD is the loss of dopaminergic neurons in the SN 39, 40. PQ is believed to cause a loss of dopaminergic neuron in SN through generating oxidative- and proinflammatory stress. Mutation in or over expression of α-synuclein is thought to be a major cause of formation of intracellular protein aggregates or Lewy body 32, 39-41. Physical interaction of paraquat with α- synuclein was also shown to help insoluble fibril formation 41. We showed that treatment with AZD restored the lost dopamine neurons as well as reduced α-synuclein levels in SN and ameliorated PD symptoms in mice model of PD we developed (Fig. 2C). Importantly, the ameliorating effect was correlated with elevated levels of HSP70 in SN (fig. 2C). In fly models as well AZD induced HSF1 activity and ameliorated the eye defect caused by expression of protein with an expanded polyQ tract (Fig. 2F-H) 42. Data support that major effect of AZD is mediated through HSF1 activation rather than its antioxidant property. AZD did not show any free radical scavenging in DPPH and DCFH-DA assay (figs. S10AB). Furthermore, AZD was reported to have relatively weak anti-inflammatory activity compared to other triterpenoids 19, 43. Finally, AZD identified by this study is one of a kind that interacts with HSF1 with high specificity and enhances HSE interaction by HSF1. No interference with HSP90 and proteasome function also support the idea that AZD would show less toxicity in animals as supported by SGOT and SGPT tests. The results are consistent with model that AZD sequester the free pool of HSF1 that is normally in dynamic equilibrium with different repressive complexes with its basal activity to convert the species to active conformation. It is yet not understood the consequence of interruption of this dynamic equilibrium in long term. Future study should be aimed to understand this including global effect on a cell on exposure to AZD. Overall our results show a great prospect with AZD as a lead molecule to develop long desired small molecule therapeutics for NDs which take a heavy toll on our society. AZD is also should be valuable to better understand mechanism of HSF1 function.

References

1.H. T. Orr and H. Y. Zoghbi, Annu Rev Neurosci, 2007, 30, 575-621.
2.J. R. Gatchel and H. Y. Zoghbi, Nat Rev Genet, 2005, 6, 743-755.
3.D. W. Neef, A. M. Jaeger and D. J. Thiele, Nat Rev Drug Discov, 2011, 10, 930-944.
4.M. R. Cookson, Nat Rev Neurosci, 2010, 11, 791-797.
5.J. Labbadia and R. I. Morimoto, Annu Rev Biochem, 2015, 84, 435-464.
6.M. Maheshwari, S. Bhutani, A. Das, R. Mukherjee, A. Sharma, Y. Kino, N. Nukina and N. R. Jana, Hum Mol Genet, 2014, 23, 2737-2751.
7.P. K. Auluck and N. M. Bonini, Nat Med, 2002, 8, 1185-1186.
8.D. W. Neef, M. L. Turski and D. J. Thiele, PLoS Biol, 2010, 8, e1000291.
9.A. Ali, S. Bharadwaj, R. O'Carroll and N. Ovsenek, Mol Cell Biol, 1998, 18, 4949-4960.
10.S. Bharadwaj, A. Ali and N. Ovsenek, Mol Cell Biol, 1999, 19, 8033-8041.
11.Y. Shi, D. D. Mosser and R. I. Morimoto, Genes Dev, 1998, 12, 654-666.
12.J. Zou, Y. Guo, T. Guettouche, D. F. Smith and R. Voellmy, Cell, 1998, 94, 471-480.
13.I. Shamovsky and E. Nudler, Cell Mol Life Sci, 2008, 65, 855-861.
14.I. Shamovsky and E. Nudler, Sci STKE, 2006, 2006, pe40.
15.M. Vera, B. Pani, L. A. Griffiths, C. Muchardt, C. M. Abbott, R. H. Singer and E. Nudler, Elife, 2014, 3, e03164.
16.H. McDonough and C. Patterson, Cell Stress Chaperones, 2003, 8, 303-308.
17.K. R. Brandvold and R. I. Morimoto, J Mol Biol, 2015, 427, 2931-2947.
18.B. Calamini, M. C. Silva, F. Madoux, D. M. Hutt, S. Khanna, M. A. Chalfant, S. A. Saldanha, P. Hodder, B. D. Tait, D. Garza, W. E. Balch and R. I. Morimoto, Nat Chem Biol, 2012, 8, 185-196.
19.A. Alam, S. Haldar, H. V. Thulasiram, R. Kumar, M. Goyal, M. S. Iqbal, C. Pal, S. Dey,
S. Bindu, S. Sarkar, U. Pal, N. C. Maiti and U. Bandyopadhyay, J Biol Chem, 2012, 287, 24844-24861.
20.M. Raghavendra, R. Maiti, S. Kumar and S. Acharya, International journal of applied & basic medical research, 2013, 3, 37-47.
21.D. D. Mosser, N. G. Theodorakis and R. I. Morimoto, Mol Cell Biol, 1988, 8, 4736-4744.
22.N. Neznanov, A. V. Gorbachev, L. Neznanova, A. P. Komarov, K. V. Gurova, A. V. Gasparian, A. K. Banerjee, A. Almasan, R. L. Fairchild and A. V. Gudkov, Cell Cycle, 2009, 8, 3960-3970.
23.J. Anckar and L. Sistonen, Annu Rev Biochem, 2011, 80, 1089-1115.

24.S. D. Westerheide, J. D. Bosman, B. N. Mbadugha, T. L. Kawahara, G. Matsumoto, S. Kim, W. Gu, J. P. Devlin, R. B. Silverman and R. I. Morimoto, J Biol Chem, 2004, 279, 56053-56060.
25.J. M. Solomon, J. M. Rossi, K. Golic, T. McGarry and S. Lindquist, New Biol, 1991, 3, 1106-1120.
26.D. D. Mosser, A. W. Caron, L. Bourget, C. Denis-Larose and B. Massie, Mol Cell Biol, 1997, 17, 5317-5327.
27.M. Akerfelt, R. I. Morimoto and L. Sistonen, Nat Rev Mol Cell Biol, 2010, 11, 545-555.
28.G. Wang, N. Sawai, S. Kotliarova, I. Kanazawa and N. Nukina, Hum Mol Genet, 2000, 9, 1795-1803.
29H. Yang, D. Chen, Q. C. Cui, X. Yuan and Q. P. Dou, Cancer Res, 2006, 66, 4758-4765.
30.P. K. Auluck, H. Y. Chan, J. Q. Trojanowski, V. M. Lee and N. M. Bonini, Science, 2002, 295, 865-868.
31.J. A. Obeso, M. C. Rodriguez-Oroz, C. G. Goetz, C. Marin, J. H. Kordower, M. Rodriguez, E. C. Hirsch, M. Farrer, A. H. Schapira and G. Halliday, Nat Med, 2010, 16, 653-661.
32.S. Mitra, N. Chakrabarti and A. Bhattacharyya, Journal of neuroinflammation, 2011, 8, 163.
33.D. D. Mosser, P. T. Kotzbauer, K. D. Sarge and R. I. Morimoto, Proc Natl Acad Sci U S A, 1990, 87, 3748-3752.
34.S. G. Ahn and D. J. Thiele, Genes Dev, 2003, 17, 516-528.
35.S. K. Rabindran, R. I. Haroun, J. Clos, J. Wisniewski and C. Wu, Science, 1993, 259, 230-234.
36.S. Yanpallewar, S. Rai, M. Kumar, S. Chauhan and S. B. Acharya, Life Sci, 2005, 76, 1325-1338.
37.C. A. Patwardhan, A. Fauq, L. B. Peterson, C. Miller, B. S. Blagg and A. Chadli, J Biol Chem, 2013, 288, 7313-7325.
38.O. Littlefield and H. C. Nelson, Nat Struct Biol, 1999, 6, 464-470.
39.C. Berry, C. La Vecchia and P. Nicotera, Cell Death Differ, 2010, 17, 1115-1125.
40.M. G. Purisai, A. L. McCormack, S. Cumine, J. Li, M. Z. Isla and D. A. Di Monte,
Neurobiol Dis, 2007, 25, 392-400.
41.A. B. Manning-Bog, A. L. McCormack, J. Li, V. N. Uversky, A. L. Fink and D. A. Di Monte, J Biol Chem, 2002, 277, 1641-1644.
42.P. Kazemi-Esfarjani and S. Benzer, Science, 2000, 287, 1837-1840.
43K. Ilango, G. Maharajan and S. Narasimhan, Nat Prod Res, 2013, 27, 1463-1467.
44.M. C. Ellis, E. M. O'Neill and G. M. Rubin, Development, 1993, 119, 855-86